Sustainable Structures
ISSN: 2789-3111 (Print); ISSN: 2789-312X (Online)
http://www.sustain-dpl.com/journal/sust
DOI: 10.54113/j.sust.2026.000118

ORIGINAL ARTICLE

Experimental investigation of the effect of activated bamboo biochar blended cement on concrete properties

Afan Tamboli[a,*], Sabir Sayyed[b], Mayur Maske[b], Savita Patil[b], Sourabh Patil[a]

[a]Department of Civil Engineering, Kasegaon Education Society's Rajarambapu Institute of Technology, Affiliated to Shivaji University, Sakhrale, India
[b]Department of Civil Engineering, Kasegaon Education Society's Rajarambapu Institute of Technology, Affiliated to Shivaji University, Sakhrale, India
[*]Corresponding Author: Afan Tamboli. Email: afantamboliat5@gmail.com

Abstract: This study examined the effect of incorporating activated bamboo biochar into cement on concrete properties. Bamboo biochar, a carbon-rich material produced through pyrolysis, was used to replace cement at 0%, 5%, 10%, and 15% by weight in M20 grade concrete mix. This study evaluated the carbon sequestration capacity, physical and mechanical properties of pure and blended cement, properties of fresh and hardened concrete, and economic viability. The results showed that increasing the biochar content significantly enhanced CO_2 sequestration, with a maximum uptake of 49.05% at 15% replacement. However, higher biochar content increased the standard consistency, setting times, and water absorption, while decreasing the compressive strength. The 5% biochar mix slightly outperformed the control in terms of compressive and split tensile strengths, but higher percentages reduced these properties. The impact strength, ultrasonic pulse velocity, and water penetration tests also decreased with increasing biochar content. Microstructural analysis revealed higher carbon content but decreased levels of other elements with increased biochar. Economic analysis showed higher costs for biochar concrete mixes because of the higher unit cost of the biochar. Despite the increased expenses, integrating biochar into concrete offers significant environmental benefits, presenting a transformative innovation for sustainable construction.

Keywords: bamboo biochar, cement replacement, carbon sequestration, low carbon concrete, sustainable material

1 Introduction

The cement industry is a significant contributor to global carbon emissions, accounting for 5-8% of total emissions. This industry is expanding, particularly in emerging economies, and CO2 emissions are expected to increase by 4% by 2050. The main factors contributing to these emissions are fuel burning and electricity consumption during the production process [1]. Interestingly, although efforts are being made to reduce emissions, some novel processes may yield mixed results. For instance, a process for producing cement by recycling used concrete and mortar has shown higher energy consumption but lower carbon dioxide emissions than traditional Portland cement production [2]. Additionally, carbon dioxide uptake due to mortar and concrete carbonation is now being considered in emission calculations, which could significantly impact reported emissions [3]. Several strategies have been explored to address this issue. These include material substitution [4], machine learning algorithms

Received: 24 December 2025; Received in revised form: 4 July 2026; Accepted: 8 July 2026

for more efficient carbon accounting [5], and the use of geopolymer materials as alternatives to traditional cement [6]. The optimal combination of low-carbon measures could potentially reduce annual emissions by approximately 65% in 2050 and cumulative emissions by approximately 48% from to 2020-2050 in developing countries [7]. An integrated approach combining Carbon Capture and Storage (CCS), supplementary cementitious materials (SCMs), and nanotechnology has also been proposed as a promising solution for sustainable cement production [8].

Biochar is a carbon-rich solid material produced via the thermochemical conversion of biomass in an oxygen-restricted environment [8, 9]. It is typically created by heating organic matter, such as plant- and animal-based biomass, under low- or no-oxygen conditions [10, 5]. This pyrolysis process produces a stable carbon-rich substance with various beneficial properties [11]. Biochar has emerged as a promising sustainable substitute for cement in the production of concrete. This innovative approach offers opportunities for environmental sustainability and resource conservation in the construction industry [12]. Recent studies have shown that incorporating biochar into concrete enhances its mechanical properties, durability, and environmental performance. The potential of biochar as a cement replacement stems from its ability to improve concrete strength and other properties when added in small amounts, typically ranging from 0.08% to 5% [13]. Interestingly, some studies have explored even higher replacement levels, with one study incorporating up to 25% biochar by weight as a substitute for both OPC and quartz sand in ultra-high-performance fiber-reinforced concrete (UHPC) [14]. The optimal dosage of bamboo biochar in concrete appears to be between 1--3% by weight of cement, which can improve compressive strength, fracture toughness, and crack resistance [15]. The use of biochar in concrete not only addresses the environmental concerns associated with cement production but also offers a solution for agricultural waste management. In Saudi Arabia, date palm waste has been successfully converted to biochar and used as an additive in high-strength concrete [16]. Similarly, rice straw biochar has shown promising results in improving the properties of concrete [17]. Activated biochar typically undergoes chemical activation processes, such as KOH activation, which enhance its surface area and porosity. This enhancement increases the adsorption capabilities and reactivity of the material, making it effective in various applications, including environmental remediation. For concrete applications, activated biochar is believed to positively influence the hydration process and microstructure development in cement mixtures, potentially improving mechanical properties, such as compressive and flexural strength, under optimal conditions [12]. Ordinary biochar, on the other hand, provides benefits in terms of sustainability and resource conservation. It can serve as a partial substitute for cement, thereby reducing the CO_2 emissions associated with cement production. The role of ordinary biochar primarily includes enhancing the durability of concrete by reducing the carbonation depth and chloride ion penetration, with its fineness and dosage playing critical roles in determining the extent of these improvements [12]. The overall effectiveness of biochar in concrete depends on several factors, including its activation process, fineness, and proportion used in the mix. Activated biochar, due to its increased surface area, may offer better enhancements in strength and durability compared to ordinary biochar. However, both forms contribute to enhanced environmental sustainability and reduced carbon footprints in construction practices by partially replacing traditional cement components [13]. The research gap regarding biochar replacement ratios exceeding 8% has been explicitly identified by researchers such as Turovaara et al. [18], who noted: "It has been noted that there is a lack of studies regarding larger replacement ratios (>8%) of biochar in concrete," providing direct scientific justification for investigating higher dosage levels. Comprehensive literature review reveals that the 0-5% range is extensively validated as optimal for mechanical performance [19, 12, 20], with 5% emerging as a critical threshold across multiple independent studies examining bamboo biochar, wood biochar, and agricultural waste-derived biochars [21, 22, 23]. The use of 5% incremental steps---a standard methodology in dose-dependent material research---enables systematic detection of non-linear performance trends, identification of optimal dosage thresholds, and direct comparison with existing literature spanning concrete, mortar, and cementitious composites[12, 24]. Specifically, Gunasekaran et al. [25] recently demonstrated the viability of 0%, 5%, 10%, and 15% bamboo biochar replacement in concrete, establishing 10% as optimal for compressive strength (59.2 MPa) and 5% for flexural strength (7.8 MPa), while simultaneously achieving enhanced CO_2 sequestration. This introduction establishes critical research gaps for activated bamboo biochar specifically: (i) extensive studies limited to $\leqslant$ 8% cement replacement, with very few investigations beyond 8% for activated bamboo biochar specifically, (ii) lack of comprehensive CO_2 uptake testing for high-dosage activated bamboo biochar, and (iii) absence of economic feasibility analysis for activated bamboo biochar concrete.

Therefore, this study employs 0%, 5%, 10%, and 15% activated bamboo biochar replacement in M20 concrete—a scientifically defensible, literature-informed experimental design addressing the identified gaps. The research methodology comprised three main phases. First, the influence of biochar on cement properties was examined. Second, the fresh, hardened, and durability properties of concrete incorporating biochar were analyzed, along with microstructural analysis. Finally, environmental and economic feasibility were assessed through carbon uptake and cost analyses, respectively. Through a comprehensive analysis of the results, this study aims to contribute to the development of eco-friendly construction materials that not only mitigate the environmental impact of concrete production but also promote the effective utilization of agricultural waste products. The findings of this study have the potential to pave the way for sustainable construction practices, support developmental goals, and enhance material performance in the construction industry.

2 Methods and Materials

2.1 Materials

Ordinary Portland Cement (OPC) of 43 grade from the JK Super brand was used. It has a specific gravity of 3.15. The fine aggregate (sand) had a specific gravity of 2.70, and its zone was I. The specific gravity of the coarse aggregates was 2.90.

Activated bamboo biochar was procured from BISJ Exporters, Chandigarh, India, produced through high-temperature pyrolysis at 900–1000°C and activated using steam treatment without any chemical activators. This physical activation enhanced the internal structure by increasing pore volume and surface area. The material was ground to a fine powder and characterized using multiple standardized testing methods, and the corresponding results are summarized in **Table 1**. Particle size distribution analysis was performed using laser diffraction (ISO 13320:2020) with a Malvern Mastersizer 3000 instrument, revealing that 90% of particles pass through a 75 µm sieve with a mean particle size of approximately 20 µm, comparable to Ordinary Portland Cement (OPC 43). The specific surface area was determined through nitrogen adsorption isotherms at 77 K following ASTM D6556-17 standards, with samples degassed at 250°C for 4 hours prior to measurement; the material exhibits a BET specific surface area in the range of 350–550 m^2/g. Pore size distribution was determined using the Brunauer-Joyner-Halenda (BJH) method (ASTM D4641-15), revealing an average pore size of approximately 2–3 nm with predominantly microporous character (pores <2 nm) and cumulative micropore volume of 0.15–0.25 cm^3/g, complemented by larger macropores ranging from 10–200 µm attributed to the preserved bamboo vascular structure. Surface elemental composition determined using Energy Dispersive Spectroscopy (EDS) confirmed carbon content of approximately 75% and oxygen content of approximately 25%. As shown in **Fig. 1 (a, b)**, the SEM image displays a highly porous structure with visible honeycomb-like voids and interconnected pores characteristic of the multi-scale porous morphology. This multi-scale porous morphology provides a high surface area, enhancing both water absorption and CO_2 adsorption capacity of the biochar in cementitious applications.

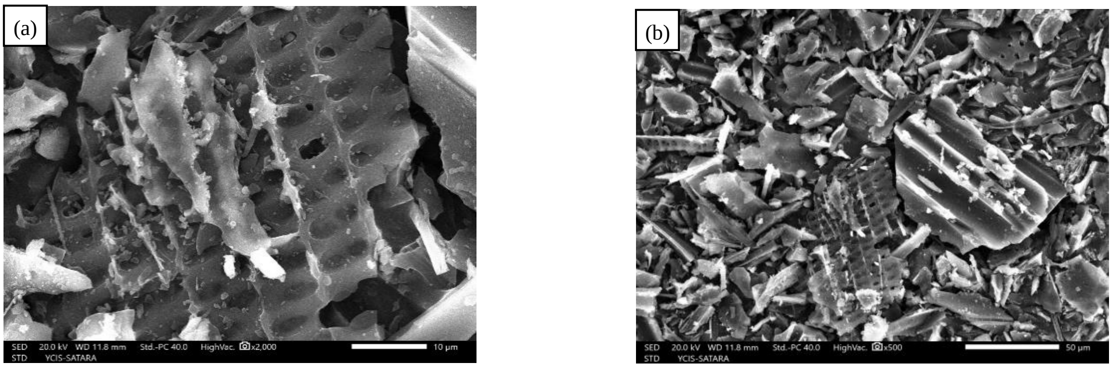

Fig. 1. SEM image of activated bamboo biochar (a) 10 µm (b) 50 µm

Table 1. Properties of activated bamboo biochar

Specific gravity	pH	Moisture content (%)	Carbon (Mass %)	Oxygen (Mass %)	Surface area (m^2/g)	Pore volume (cm^3/g)	Average particle size (μm)
1.71	9.75	0-3	75.40	24.60	350-550	0.15-0.25	20

2.2 Mix Design and Preparation of Specimens

In this study, bamboo biochar was used to replace cement by weight at 0%, 5%, 10%, and 15% in an M20 grade concrete mix designed as per IS 10262:2019 [26], while the remaining constituents were kept constant, as presented in **Table 2**. The mixtures were designed with a constant water-to-binder ratio (*w*/*b*) of 0.50 for all mixes, where the binder consists of the combined mass of cement and biochar. As the biochar content increased from M0 to M15, the cement content was reduced proportionally, while the total binder content and water dosage remained constant; therefore, although the nominal water-to-cement ratio (*w*/*c*) increases with higher biochar contents, the overall *w*/*b* ratio is unchanged across all mixes. No chemical admixtures, including plasticizers or superplasticizers, were used in any mix in order to isolate the intrinsic effect of activated bamboo biochar on the fresh and hardened properties of concrete.

Table 2. Proportion of materials in different concrete mixes

Material	M0 (0% biochar)	M5 (5% biochar)	M10 (10% biochar)	M15 (15% biochar)
Cement (kg/m^3)	372	353	334	315
Biochar (kg/m^3)	0	19	38	57
Fine aggregate (kg/m^3)	741	741	741	741
Coarse aggregate (kg/m^3)	1194	1194	1194	1194
Water (kg/m^3)	186	186	186	186
Water to cement ratio (*w*/*c*)	0.5	0.53	0.56	0.59
Water to binder ratio (*w*/*b*)	0.5	0.5	0.5	0.5

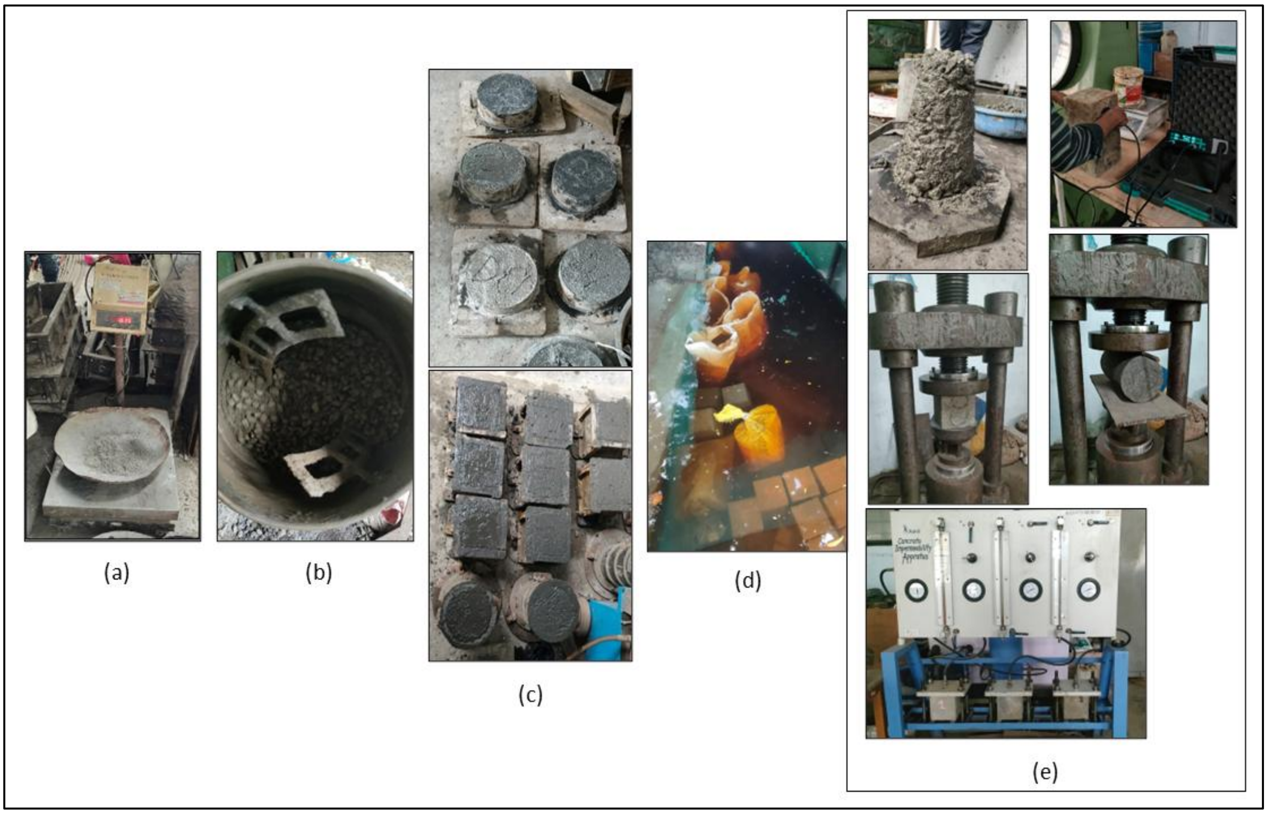

Fig. 2. (a) Weight batching (b) Mechanical mixture (c) Casted specimens (d) Curing of specimens in tank (e) Testing of specimens by using different apparatus

The specimen preparation and testing workflow adopted in this study is illustrated in **Fig. 2**. The procedure began with proportioning all constituent materials through weight batching, followed by thorough mechanical mixing to achieve a homogeneous blend. The fresh mix was then placed into moulds and manually compacted to eliminate entrapped air. Three specimen geometries—cubes, cylinders, and discs—were prepared based on the requirements of each test. **Table 3** summarises the types of tests conducted, the number of specimens used, their respective dimensions, and the testing ages. All specimens were demoulded after 24 hours and subsequently cured to the designated ages of 7, 28, 90, and 120 days; for ages beyond 28 days, specimens underwent water curing initially and were then stored in air until testing. For the cement composite mixes, biochar was incorporated as a partial replacement of cement at levels of 0%, 5%, 10%, and 15%, consistent with the replacement strategy used for the concrete mixtures.

2.3 Statistical Analysis

All concrete property tests were conducted with triplicate specimens (n = 3) for each mix design at each curing age to ensure statistical validity and reproducibility of results. Results are presented as mean ± standard deviation. The coefficient of variation (COV), calculated as (standard deviation/mean) × 100%, was used to assess test precision, with values below 5% indicating excellent reproducibility and values below 10% considered acceptable per ASTM C39 guidelines. One-way analysis of variance (ANOVA) was performed to assess statistical significance of differences among mix designs, with $p < 0.05$ considered statistically significant. Post-hoc pairwise comparisons using Student's t-test with Bonferroni correction were conducted when ANOVA indicated significant effects. Statistical analyses were performed using appropriate software, following established practices in concrete research.

Table 3. Testing matrix for cementitious mixtures

Performed on	Tests	No of specimens/trials for each mix	Dimensions (mm)	Testing Age (days)
Cement-biochar composite	Standard consistency	3	-	-
	Initial and final setting time	3	-	-
	Soundness	3	-	-
	Water absorption	3	70.6 × 70.6 × 70.6	28
Mortar	CO2 Sequestration	3	70.6 × 70.6 × 70.6	1
	Compressive strength	3	70.6 × 70.6 × 70.6	28
Concrete	Workability	1	-	-
	Hardened density	3	150 × 150 × 150	7, 28, 90, 120
	Compressive strength	3	150 ×1 50 × 150	7, 28, 90, 120
	Split tensile strength	3	300 (height) ×1 50 (diameter)	7, 28, 90, 120
	Impact strength	3	150 (diameter) × 63(thickness)	7, 28, 90, 120
	Ultrasonic pulse velocity	3	150 × 150 × 150	28
	Water permeability	1	150 × 150 × 150	28
	Carbonation	1	300 (height) × 150 (diameter)	120
	Scanning Electron Microscope (SEM)	1	-	90
	Energy Dispersive X-ray Spectroscopy (EDS)	1	-	90

2.4 Test Methods

2.4.1 Cement biochar composite

Tests were conducted to compare the properties of the cement-biochar composites in terms of consistency, setting time, soundness, water absorption, and compressive strength (mortar). All tests, except for water absorption, were conducted according to the IS 4031:1988 standards [27]. Water absorption was measured according to IS 2185 (Part 1) 2005 [28].

2.4.2 Workability

The workability of the biochar concrete was assessed using a slump test according to IS 1199:1959 [29]. A standard slump cone was filled with fresh concrete in three layers; each compacted with 25 strokes using tamping rods. The cone was lifted, and the vertical height (slump) was measured.

2.4.3 Hardened properties of biochar concrete

The hardened density and compressive strength were determined according to IS 516:1959 [30] on 150 mm cured concrete cubes. The split tensile strength was evaluated using cylindrical specimens (150 mm diameter and 300 mm height) as per IS 5816:1999 [31]. Impact strength was assessed using the drop-weight test on discs 150 mm in diameter and 63 mm in height, and the number of blows at first and total failures was measured [32]. Ultrasonic Pulse Velocity (UPV) testing was conducted according to IS 13311 (Part 1) 1992 [33].

2.4.4 Durability properties of biochar concrete

The water penetration depth was tested on 150 mm cubes after 28 d. The cubes were maintained for three days at 1, 3, and 5 kg/cm². The carbonation depth was measured by spraying a phenolphthalein solution on 120-day cured cylinders and observing the depth of carbonation according to IS 516 (Part 5/Section 3) 2021 [34].

2.4.5 Microstructural analysis of biochar concrete

Microstructural analysis was performed using Scanning Electron Microscopy (SEM) and Energy-Dispersive X-Ray Spectroscopy (EDS) on 90 days of biochar concrete powder, which helped examine its microstructure and elemental composition.

2.4.6 Carbon uptake capacity of cement biochar composite

An accelerated carbonation chamber was developed to evaluate the carbon-uptake capacity of the cement-biochar composites, as shown in **Fig. 3**, with its specifications detailed in **Table 4**. Cubes measuring 70.6 mm were cast and allowed to cure for 24 hours. After curing, the cubes were dried to a consistent moisture state to ensure uniform initial conditions and then placed into the carbonation chamber. CO_2 was injected to create a CO_2-saturated environment.

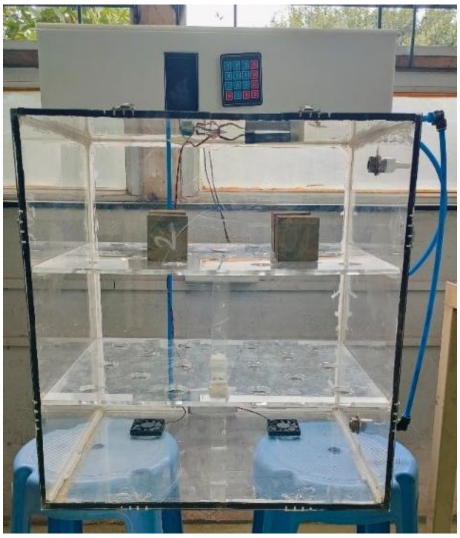

Fig. 3. Accelerated carbonation chamber

After the initial injection, the CO_2 flow was stopped, and the chamber was sealed again kept for 24 hours to allow carbonation reactions to occur between CO_2, calcium hydroxide produced from cement hydration, and biochar surfaces. The CO_2 concentration was measured at three stages—initial, peak, and final—under controlled environmental conditions, with temperature maintained between 25 and 28 °C and relative humidity regulated within 50 to 70%. For each biochar replacement percentage, three cubes were prepared and tested, and the average value was taken to ensure reproducibility. This procedure was inspired by similar studies by Nair et al. [35] and Sacdalan et al. [21], and the CO_2

sequestration capacity was calculated using the following formula:

$$Carbon\ uptake\left(100\%\right) = \frac{Peak - Final}{Peak - Ininal} \times 100\% \tag{1}$$

Table 4. Specifications of CO_2 carbonation chamber

Parameter	Description
Internal Dimensions	600 mm × 600 mm × 450 mm
Chamber Volume	162 L
Material	Acrylic
Temperature range	0–50 °C
Relative Humidity Control Range	20–95%
CO_2 Concentration Control	0-50000 ppm
Sealing Mechanism	Gas-tight, manual locking
Air Circulation	Built-in fan for uniform CO_2 distribution
Data Logging	Digital sensors for temperature, humidity and CO_2

3 Results and Discussion

3.1 Cement biochar composite properties

Table 5 shows the test results for cement-biochar mixes, where biochar replaced cement at levels of 0%, 5%, 10%, and 15% (denoted as C0, C5, C10, and C15, respectively), and were analyzed in comparison to the control mix (C0). The standard consistency increased from 33% in C0 to 45% in C15, with percentage increases of 9.1, 30.3, and 36.4% for C5, C10, and C15, respectively. These values are within the acceptable ranges for cement pastes, as per IS 4031 (Part 4), which stipulates that the standard consistency typically falls between 25% and 45%. The increasing demand for water with a higher biochar content reflects the impact of the porous structure of the biochar on water retention.

The initial and final setting times also increased progressively with increasing biochar content. The initial setting time increased from 35 min for C0 to 49 min for C15, and the final setting time increased from 300 min for C0 to 405 min for C15. These increments align with IS 4031 (Part 5), which specifies a minimum initial setting time of 30 min and a maximum final setting time of 600 min for ordinary Portland cement. The delay in the setting times with higher biochar replacement suggests that biochar modifies the hydration process and slows down the reaction kinetics.

Table 5. Summary of tests on cement biochar composite

Test	Mix ID			
	C0	C5	C10	C15
Standard consistency (%)	33	36	43	45
Initial setting time (min)	35	40	42	49
Final setting time (min)	300	330	412	405
Soundness (mm)	0.1	0.1	0.2	0.1
Water absorption (%)	13.48	20.72	24.41	29.23
Compressive strength on mortar (N/mm^2)	42.38	41.08	33.73	33.35

The soundness remained relatively stable, with values of 0.1 mm for C0, C5, and C15, and slightly increased to 0.2 mm for C10. These values comply with IS 4031 (Part 3), which sets the permissible limit for soundness at a maximum of 10 mm, indicating that biochar incorporation does not adversely affect the dimensional stability of the pastes. However, water absorption exhibited a significant increase from 13.48% in C0 to 29.24% in C15, with percentage increases of 53.7, 81.1, and 116.9% for C5, C10, and C15, respectively. The compressive strength of the paste showed a notable decline, decreasing from 42.39 MPa in C0 to 33.35 MPa in C15, with reductions of 3.1%, 20.4%, and 21.3% for C5, C10, and C15, respectively. IS 269 specifies that the minimum compressive strength for OPC 43-grade cement at 28 days should be at least 43 N/mM10. The reduction in strength with higher biochar replacement levels indicates that the mixtures may fall below the standard requirements for certain structural applications.

3.2 Workability

The incorporation of biochar into concrete mixtures significantly affected workability, as indicated by the slump test results. The control mix (M0) without biochar showed a slump of 30 mm, whereas the biochar-replaced mixes (M5, M10, and M15) recorded zero slump, reflecting a very stiff consistency. This reduction in workability is attributed to the high water-absorption capacity and porous structure of biochar, which reduce the amount of free water available for flow and compaction. The influence of biochar on workability depends on both its dosage and fineness, with higher replacement levels and finer particles generally causing greater loss of slump[13]. Although biochar commonly reduces flowability and ease of placement, some studies have reported beneficial effects on other fresh and early-age properties; for example, Neve et al. [36] found that biochar can reduce concrete shrinkage during curing, while Ling et al. [12] reported that biochar with a fineness of 73.28 µm had a pronounced influence on the mechanical strength and workability of concrete. In the present study, no chemical admixtures were incorporated; however, in practical applications, plasticizers or superplasticizers may be utilized to counteract the reduction in workability.

3.3 Hardened properties of biochar concrete

3.3.1 Hardened density

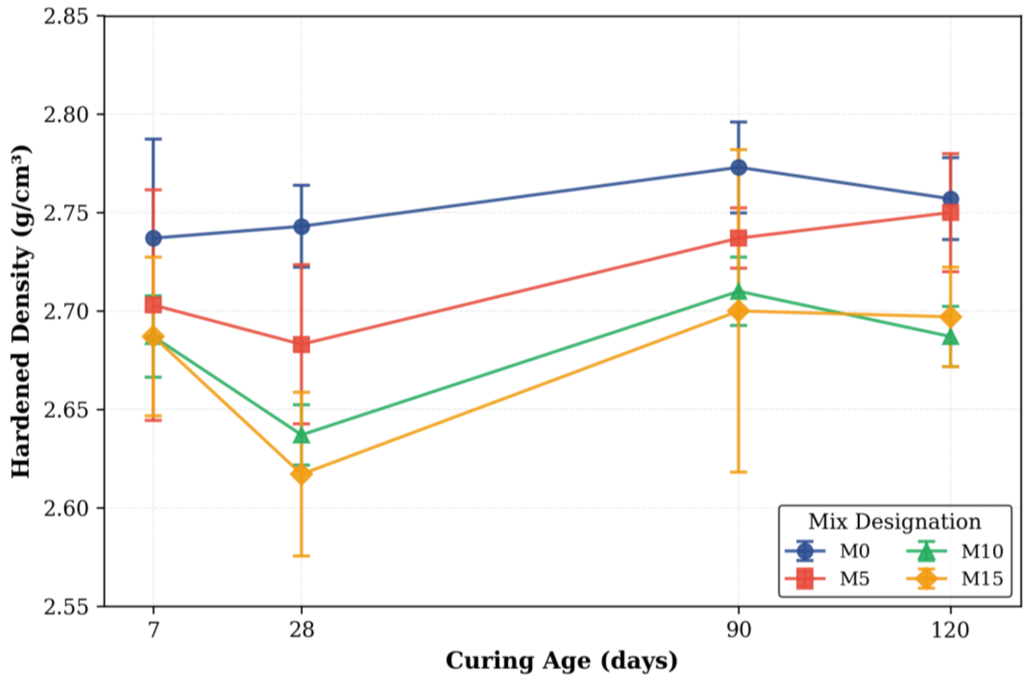

Fig. 4. Hardened density of different concrete mixes

Fig. 4 shows the development of hardened density with curing age for all concrete mixes. The control mix (M0) consistently exhibited the highest density across all ages, increasing slightly from 2.737 ± 0.050 g/cm³ at 7 days to 2.757 ± 0.021 g/cm³ at 120 days. Introduction of bamboo biochar resulted in minor reductions in density. Mix M5 showed 2.703 ± 0.059 g/cm³ at 7 days and 2.750 ± 0.030 g/cm³ at 120 days, corresponding to a minimal decrease of ~1.2% relative to M0 at the final age. Mixes M10 and M15 exhibited progressively lower densities, achieving 2.687 ± 0.015 g/cm³ and 2.697 ± 0.025 g/cm³ at 120 days, representing reductions of ~2.5% and ~2.2%, respectively. The reductions at earlier ages were smaller: at 7 days, M5, M10, and M15 decreased by approximately 1.1%, 1.8%, and 1.5%, respectively, relative to M0, while at 28 days, the decreases became more pronounced (M5: ~2.2%, M10: ~3.6%, M15: ~4.4%). At 90 days, the reductions ranged from ~1.1% (M5) to ~2.5% (M15), and by 120 days, M5 exhibited a minimal reduction (~0.4%), whereas M10 and M15 remained lower (~2.5% and ~2.2%). One-way ANOVA revealed statistically significant differences among mix designs at 28 days (F = 9.43, p = 0.0053) and 120 days (F = 7.05, p = 0.0124), while differences at 7 and 90 days were not significant ($p > 0.05$). The coefficient of variation across all measurements remained exceptionally low (<2%), indicating excellent experimental precision. Overall, the results indicate that increasing biochar content leads to a gradual decline in hardened density, with the magnitude of reduction dependent on replacement level. This trend contrasts with findings by Sinha et al. [37], who reported that incorporating biochar into cement paste increased density from 1.98 g/cm³ for the control to a maximum of 2.18 g/cm³ at 5% biochar, with a slight decrease to 2.1 g/cm³ at 10% replacement.

3.3.2 Compressive strength

Fig. 5 shows that mix M0 develops compressive strength steadily, from 20.49 ± 0.87 MPa at 7 days (coefficient of variation = 4.2%) to 33.68 ± 1.24 MPa at 120 days (coefficient of variation = 3.7%). Mix M5 achieves slightly higher strengths, increasing from 20.20 ± 0.76 MPa at 7 days to 34.30 ± 1.18 MPa at 120 days, representing a statistically significant enhancement of 1.84% compared to M0 at 120 days ($p < 0.05$), indicating that 5% biochar can enhance concrete performance, particularly at later ages. The improved strength at 5% biochar replacement can be attributed to synergistic mechanisms: (i) nucleation effect, where the high surface area of activated biochar provides nucleation sites for hydration products and accelerates C–S–H formation; (ii) Interfacial Transition Zone (ITZ) enhancement, as fine biochar particles fill micro-voids, reducing ITZ thickness and improving bonding; (iii) internal curing effect, wherein biochar's porous structure absorbs water during mixing and releases it gradually during hydration; and (iv) micro-filler effect, where biochar particles fill interstitial spaces without significantly diluting cement content. EDS results showing higher Ca and Si concentrations in M5 compared to higher replacement levels further support the formation of additional C–S–H phases.

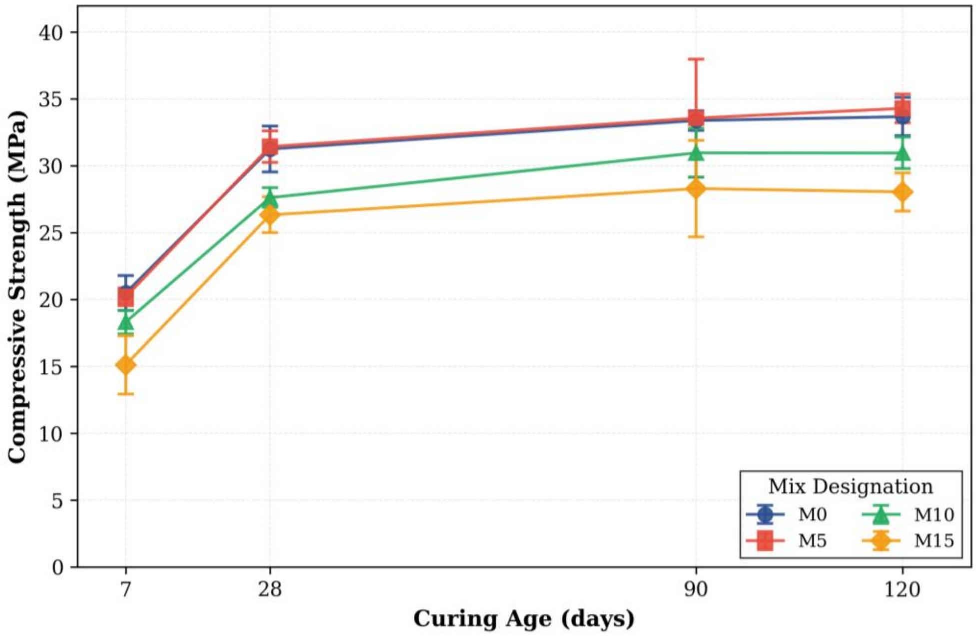

Fig. 5. Compressive strength of different concrete mixes

As the biochar content increased beyond 5%, performance declined. Mix M10 reached only 30.96 ± 1.32 MPa at 120 days, significantly lower than both M0 and M5 ($p < 0.01$), indicating that higher biochar levels may not contribute effectively to strength development. Mix M15 exhibited the lowest strengths, increasing from 15.11 ± 0.68 MPa at 7 days to only 28.05 ± 1.15 MPa at 120 days, representing a 16.7% reduction compared to M0 ($p < 0.001$), suggesting that excessive biochar disrupts bonding in the matrix. Previous studies show similar trends: woody biomass biochar at 0.50 w_t% and 2 w_t% increased 28-day strength by 16% and 9% [38]; pulp and paper mill sludge biochar at 0.1% produced strength comparable to the control [39]; and bamboo biochar mortar showed improvement at 1–3 w_t % [15]. Conversely, biochar from dry distiller grains reduced compressive strength [40], whereas replacing 5% sand with Carya cathayensis peel biochar increased strength by 16.7% [41]. Overall, biochar generally enhances compressive strength at low dosages (0.1–5%), but higher concentrations

(10–15%) may hinder performance, depending on biochar type and incorporation method.

3.3.3 Split tensile strength

Fig. 6 demonstrates that the M5 mix consistently exhibited superior tensile performance compared to the control mix (M0) and other biochar mixes across all curing periods, which is analogous to the compressive strength results. At 7 days, M5 displayed a statistically significant 14.4% increase in tensile strength relative to M0 ($p < 0.01$), attaining 2.22 ± 0.09 MPa compared to 1.94 ± 0.11 MPa for M0 (coefficient of variation = 4.1% and 5.7%, respectively). Analysis of variance results confirmed significant differences among mixes at all curing ages ($F(3,8) = 18.42$, $p < 0.001$). By 120 days, M5 tensile strength reached 3.75 ± 0.14 MPa, representing an 8.1% increase compared to M0 at 3.47 ± 0.13 MPa, indicating that 5% biochar incorporation enhanced both early-age and long-term tensile strength. These results reaffirm that moderate biochar content promotes improved mechanical performance.

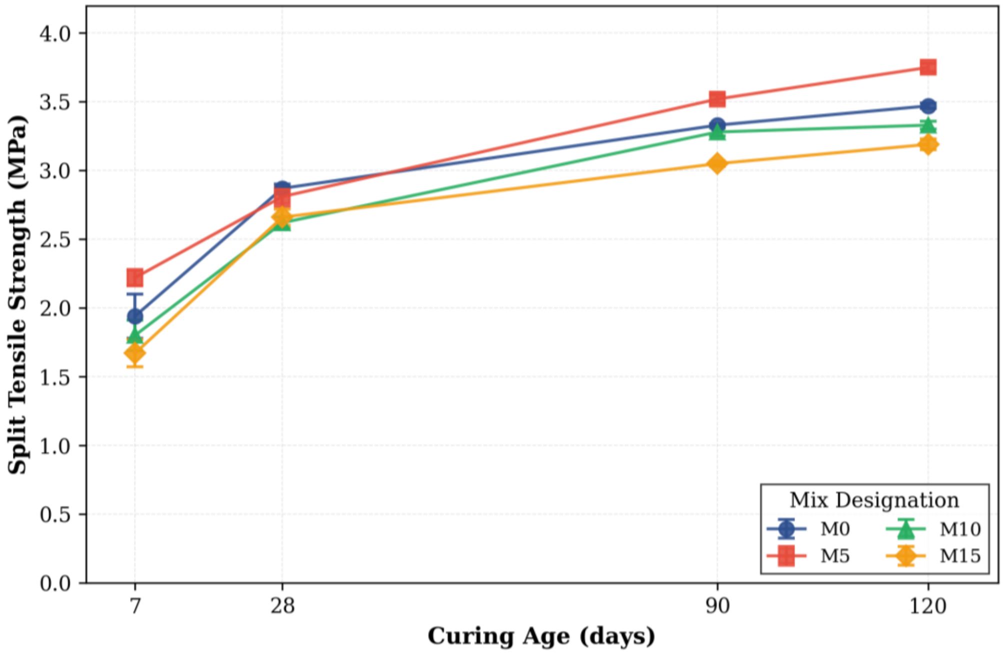

Fig. 6. Split tensile strength of different concrete mixes

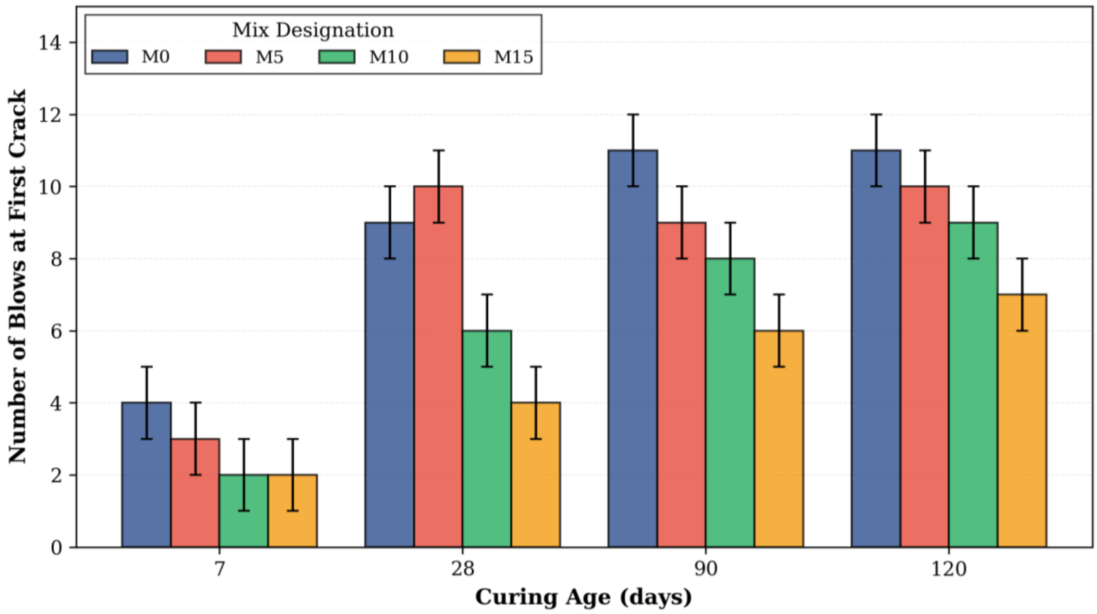

(a)

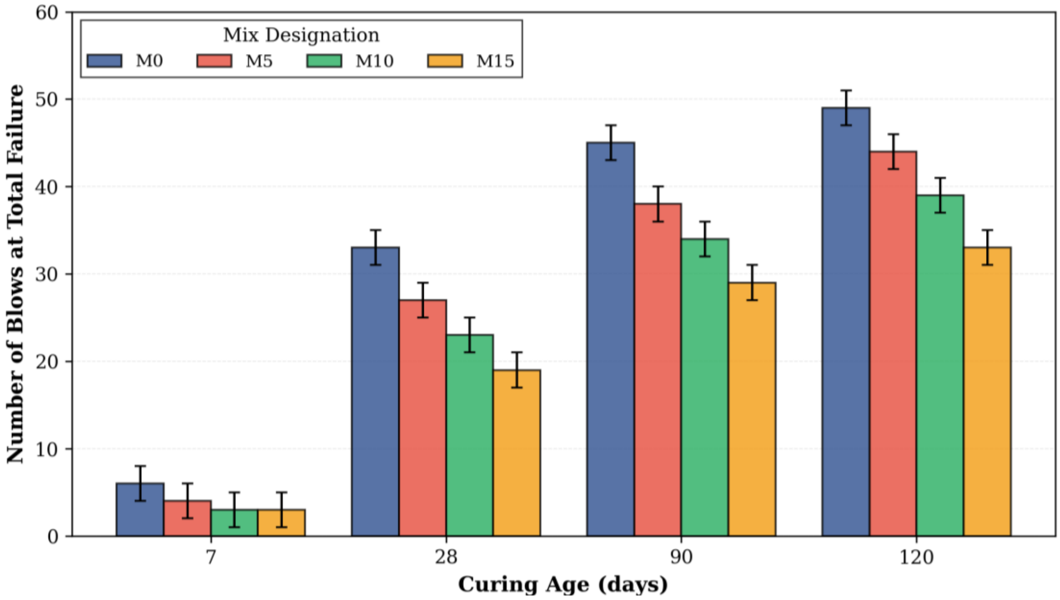

(b)

Fig. 7. (a) Average number of blows at first crack (b) Average number of blows at total failure

Conversely, the higher biochar mixes exhibited reduced performance. The M10 mix demonstrated a slight decrease, with a tensile strength of 3.33 MPa at 120 days, which was only marginally higher than that of M0. The M15 mix showed the lowest tensile strength values, starting at 1.67 MPa at 7 days and reaching 3.19 MPa at 120 days, indicating that excessive biochar disrupts the bonding between mix components and weakens the matrix. Similar observations have been reported in previous studies: Zeidabadi et al. [42] found that splitting tensile strength increased with rice husk ash up to 15% but declined at 20% due to the presence of excessive porous microaggregates, and Gupta et al. [43] noted that although 28-day compressive strength remained nearly unchanged, a reduction in split tensile strength occurred in concrete mixes containing biochar compared to control samples. Overall, these findings suggest that increased biochar content elevates porosity and diminishes bonding quality, ultimately reducing tensile strength.

Fig. 7 (a, b) presents the impact test results, showing that the control mix M0 generally exhibited the highest impact resistance at most curing ages. At 120 days, M0 required 11.0 ± 1.0 blows for first visible crack and 49.0 ± 2.0 blows for total failure. Mix M5 showed slightly reduced first-crack resistance at 10.0 ± 1.0 blows, but maintained good total failure resistance at 44.0 ± 2.0 blows. The higher biochar mixes, M10 and M15, displayed progressively reduced impact resistance, with M15 achieving only 7.0 ± 1.0 blows to first crack and 33.0 ± 2.0 blows to total failure. Analysis of variance indicated highly significant differences among mixes for both first crack ($F = 8.75$, $p < 0.01$) and total failure ($F = 35.19$, $p < 0.001$) at 120 days. The consistent standard deviations—approximately one blow for first crack and two blows for total failure—demonstrate the good reproducibility of the testing methodology.

The inclusion of biochar generally reduced impact resistance, with mixes M5, M10, and M15 showing lower values compared to M0. At 28 days, however, M5 exhibited a slight increase in impact resistance relative to M0, likely due to additional internal curing and continued hydration promoted by the biochar particles. As biochar content increased, the impact resistance progressively declined, with M15 (highest biochar content) exhibiting the lowest values. This trend may be attributed to the porous nature of biochar, which reduces matrix density and weakens interfacial bonding. Despite this reduction, all mixes showed improved impact resistance with extended curing periods, as hydration and pozzolanic reactions enhanced microstructural refinement and strength. Nevertheless, the improvement was more pronounced in the control mix, suggesting that biochar inclusion may marginally impede long-term strength development under impact loads.

3.3.4 Ultrasonic pulse velocity

Fig. 8 shows the ultrasonic pulse velocity (UPV) measurements at 28 days for all concrete mixes. The control mix M0 recorded a UPV of 3.857 ± 0.045 km/s, serving as the benchmark for comparison. Mix M5 exhibited the highest UPV value of 3.900 ± 0.020 km/s, representing a 1.1% improvement over M0, indicating enhanced microstructural density and improved interfacial transition zone (ITZ) quality, consistent with the observed mechanical property enhancements. In contrast, M10 and M15 showed slightly reduced velocities of 3.833 ± 0.025 km/s and 3.793 ± 0.035 km/s, corresponding to decreases of approximately 0.78% and 1.81%, respectively. One-way ANOVA confirmed significant differences among the mix designs (F = 5.55, p = 0.0235), and post-hoc pairwise t-tests indicated that M5 was significantly superior to M15 (p = 0.0102), while differences between M0 and biochar-incorporated mixes were not individually significant. The results suggest that small biochar additions (5%, as in M5) can slightly improve UPV by enhancing homogeneity, whereas higher contents (10% and 15%) tend to decrease UPV, likely due to increased porosity affecting wave transmission. All mixes maintained UPV values within the 3.5–4.5 km/s range, indicating good quality concrete with minimal defects [IS 13311-1992], and the remarkably low coefficient of variation (0.51–1.17%) demonstrates excellent consistency in microstructural development across replicate specimens.to 15%.

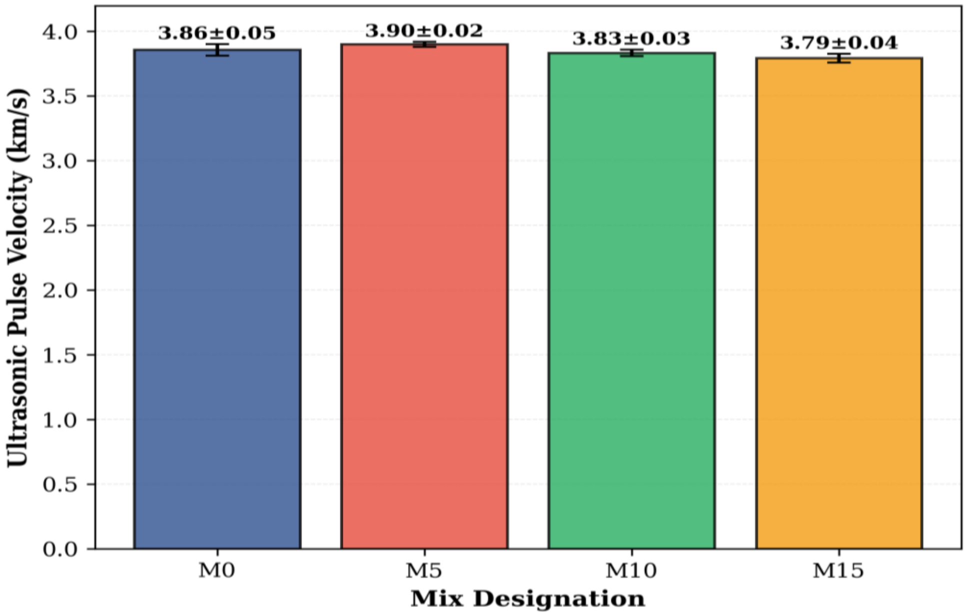

Fig. 8. Ultrasonic pulse velocity of different concrete mixes

3.4 Durability properties of biochar concrete

3.4.1 Water penetration

The results, as presented in **Fig. 9**, illustrate the variation in the water penetration depth across the different concrete mixes, with the control mix (M0) exhibiting the lowest penetration depth of 5 mm, serving as the baseline. This indicates the highest resistance to water penetration, which can be attributed to the dense and compact structure of the conventional mix. In comparison, Mix M5 demonstrated an increased penetration depth of 6 mm, representing a 20% increase in penetration depth. This suggests a slight reduction in the resistance to water penetration due to the incorporation of biochar, which may introduce minor porosity into the matrix. Mix M10 exhibited the highest water penetration depth at 7 mm, corresponding to a 40% increase compared to M0. This substantial increase indicates that a higher biochar content significantly influences the permeability of concrete, likely because of its porous nature, which increases the pathways for water ingress. Mix M15 recorded a penetration depth of 6.1 mm, reflecting a 22% increase compared to the control. Although higher than that of M0, the depth was slightly lower than that of Mix M10, suggesting that the optimized biochar content in M15 balanced the benefits and drawbacks, achieving improved performance compared to M10. Opposite results were shown in studies by Gupta et al. [38] and Gupta & Kua [44], in which the addition of biochar to concrete reduced water penetration and sorptivity, indicating higher impermeability. For instance, adding 2 wt. % biochar to concrete led to a 40% reduction in permeability, as measured by water sorptivity and water penetration tests. Fine biochar particles (0.10-2 microns) were found to be more effective in improving water tightness than coarser particles (2-100 microns), particularly under dry curing conditions[44]. These findings emphasize that although the incorporation of biochar into concrete can influence its permeability, the extent of its impact depends on the dosage and size of the biochar particles.

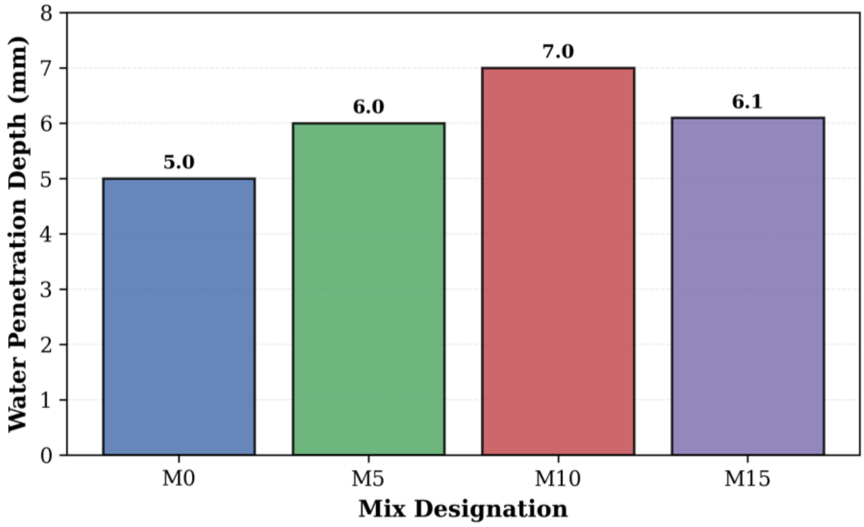

Fig. 9. Water penetration depth of different concrete mixes

3.4.2 Carbonation

The carbonation test was conducted on the concrete cylinders shown in **Fig. 10** - including both the control (M0) and biochar mixes (M5, M10, and M15) - revealed zero carbonation depth even after a 120-day exposure to atmospheric conditions (purple color from phenolphthalein indicator on concrete edges confirms the area is non-carbonated, indicating a pH above approximately 8.6–9.5 where the concrete remains alkaline).The carbonation test was performed under natural atmospheric conditions with low CO_2 concentration (approximately 400–420 ppm). The observed zero carbonation depth after 120 days suggests that the exposure period was insufficient to initiate measurable carbonation under these conditions. This carbonation process primarily depends on the diffusion of CO_2 into the concrete matrix and its subsequent reaction with calcium hydroxide to form calcium carbonate. For practical assessment of carbonation resistance, accelerated carbonation testing at elevated CO_2 concentrations (3–5% CO_2 as per EN 12390-12 or RILEM CPC-18) would provide more meaningful results within shorter timeframes.

Fig. 10. Carbonation test on concrete cylinder

3.5 Microstructural analysis of biochar concrete

Microstructural analyses were conducted using scanning electron microscopy (SEM) and energy-dispersive X-ray spectroscopy (EDS). The 90-day specimens were subjected to analysis, and the 1-micron images are presented in **Fig. 11 (a, b, c, d)**. The M5 mix exhibited a notably larger grey area, corresponding to a denser matrix with a higher abundance of calcium silicate hydrate (C-S-H) and calcium hydroxide (CH). In contrast, the M10 and M15 mixes demonstrated a pronounced increase in the black regions, indicating a greater presence of voids. Research conducted by Yang and Wang [45] obtained varied results for the XRD peaks, making it uncertain whether the addition of biochar led to an increase in the total hydration products compared with the control paste. Nevertheless, the spaces created by the incorporated biochar provided room for the formation of hydrate-containing products. Sirico et al. [22] noted a uniform distribution of biochar particles and enhanced interaction between the biochar surface and cement matrix. Furthermore, Ling et al. [12] reported that with 3% biochar addition, a micro filler effect was exhibited, resulting in more compact and uniform microstructures with additional nucleation sites for cement hydration. Increased porosity suggests reduced microstructural integrity, which negatively impacts concrete performance. This observation, supported by strength, confirms the correlation between porosity and concrete performance.

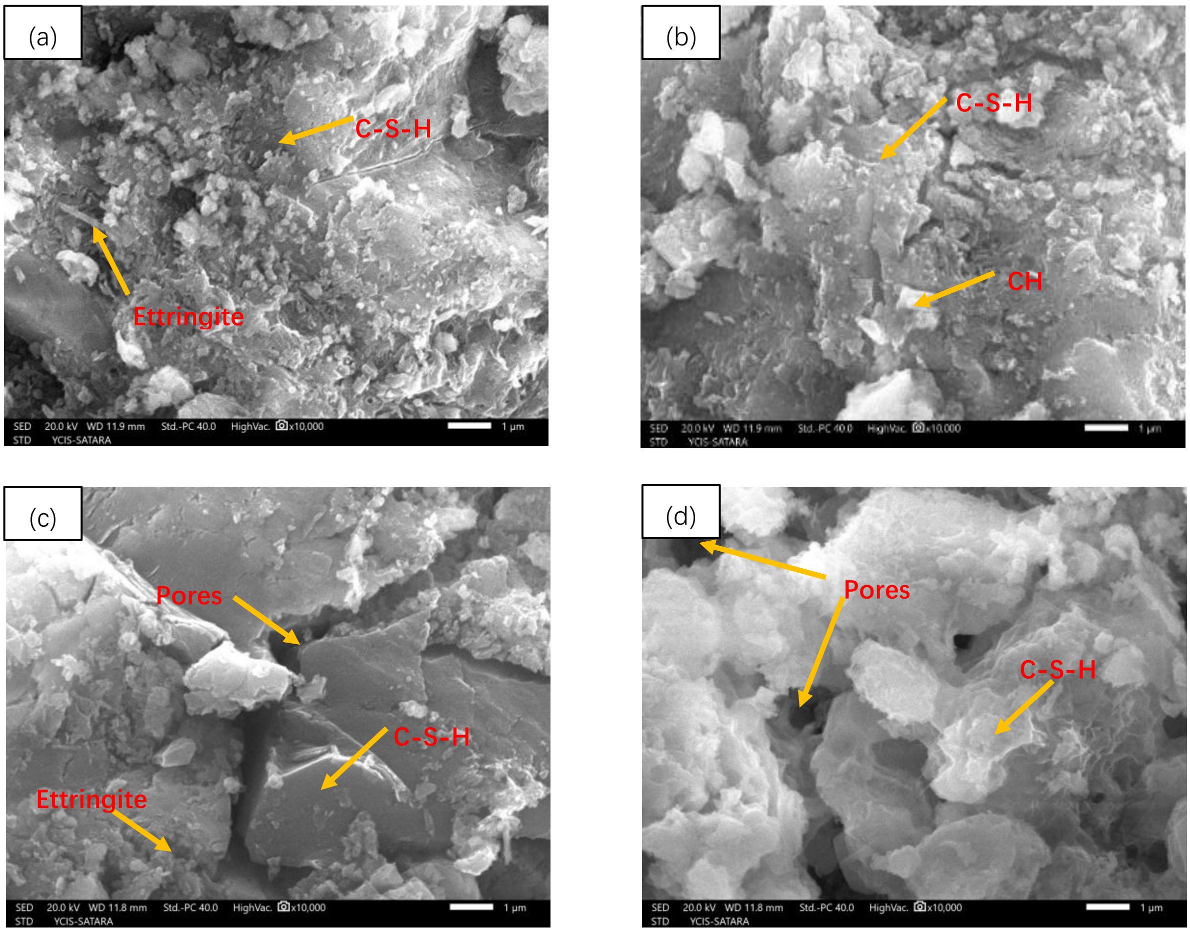

Fig. 11. SEM images (a) M0 (b) M5 (c) M10 (d) M15

The Energy Dispersive Spectroscopy (EDS) analysis presented in **Fig. 12** reveals significant compositional variations among the mixes (M0, M5, M10, and M15). M5 exhibited the highest concentrations of calcium (Ca) and silica (Si), which are essential components of cementitious materials. These elements contribute substantially to the formation of hydration products, such as calcium silicate hydrate (C-S-H), which is crucial for strength development. This observation elucidates the superior strength exhibited by M5 compared with that of the other mixes. Furthermore, the analysis indicated that as the biochar content increased across the mixes (from M5 to M15), the carbon (C) content correspondingly increased. This correlation is anticipated, given that biochar is predominantly composed of carbon. However, the increase in carbon content occurs concomitantly with a decrease in cementitious elements such as Ca and Si, potentially reducing the formation of strength-enhancing compounds and consequently leading to lower overall strength in mixes with higher biochar content (M10 and M15). This indicates that biochar primarily contributes through physical mechanisms (micro-filler effect, internal curing, nucleation) rather than chemical pozzolanic reactions.

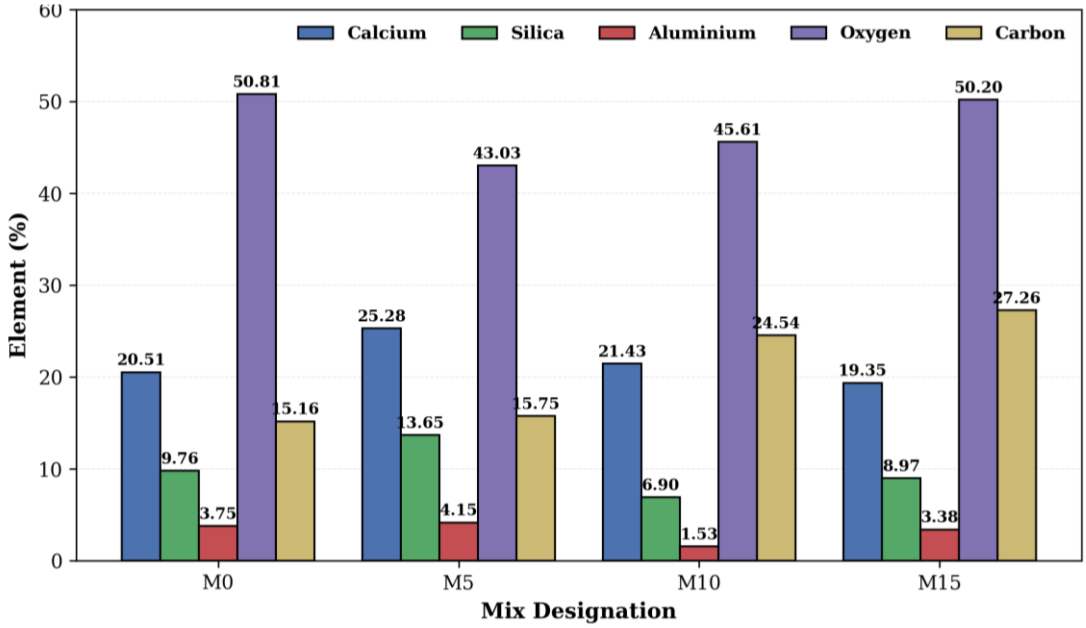

Fig. 12. Energy Dispersive Spectroscopy analysis of different concrete mixes

3.6 Carbon uptake capacity of cement biochar composite

Using the measured initial, peak, and final CO_2 concentrations presented in **Table 6** and applying Equation (1), the carbon dioxide uptake capacity of all concrete mixes was calculated. The results, illustrated in **Fig. 13**, demonstrate the remarkable sequestration potential of biochar-enhanced concrete. The control mix (M0) exhibited a baseline CO_2 uptake of 18.29 ± 1.20%, serving as the benchmark. Incorporation of bamboo biochar significantly increased carbon sequestration in a dose-dependent manner: M5 achieved 37.01 ± 0.50%, representing a 102.3% increase over M0, while M10 and M15 exhibited even higher uptake at 41.59 ± 0.18% (+127.4%) and 49.05 ± 0.13% (+168.1%), respectively. One-way ANOVA confirmed extremely significant differences among all mix designs (F = 1178.72, p < 0.000001), and post-hoc pairwise comparisons with Bonferroni correction indicated that each biochar level produced statistically distinct sequestration capacities (all pairwise p < 0.001), highlighting the robust and repeatable effect of biochar on CO_2 adsorption. Notably, the coefficient of variation decreased with increasing biochar content (M0: 6.58%, M5: 1.35%, M10: 0.43%, M15: 0.27%), indicating enhanced measurement precision and carbonation uniformity. The enhanced uptake is attributed to the porous structure of biochar, which increases surface area and provides active sites for CO_2 binding, demonstrating that even small biochar additions substantially improve the carbon sequestration potential of concrete.

Table 6. CO_2 uptake capacity of cement-biochar composites

Mix ID	Average CO_2 Concentration (ppm)			CO_2 uptake (%)
	Initial	Peak	Final	
C0	1410	18323	15230	18.29
C5	1658	13870	9350	37.01
C10	1130	20030	11980	42.59
C15	1548	17048	9450	49.05

Similar trends were observed in the studies by Nair et al. [35] and Sacdalan et al. [21]. This study found that biochar-amended mortar cubes demonstrated an increased carbon sequestration ability. In the single-candle setup, the percentage sorption of CO_2 increased from 13.66% in the control specimen to 75.30% in the 5%-biochar specimen. Similarly, in the double-candle setup, sorption increased from 8.02% for the control to 24.69% for the 5% biochar specimen [35]. The biochar content had a direct and positive impact on the CO_2 adsorption capacity of the concrete. In the single-burning candle setup, the adsorption capacity increased from 8.91% for the control mix (BC0) to 55.40% for the highest biochar content (BC8). In the double-burning candle setup, it increased from 12.97% (BC0) to 58.63% (BC8), demonstrating a consistent upward trend with increasing biochar content [21]. This experimental approach illustrates that biochar incorporation not only reduces the carbon footprint but also contributes to long-term CO_2 capture, thereby enhancing the sustainability of concrete as a construction material.

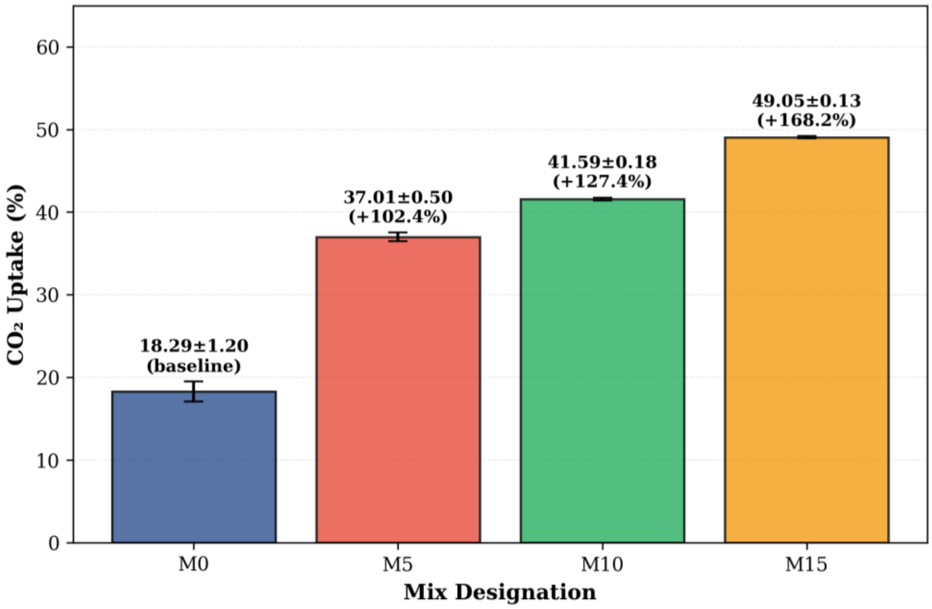

Fig. 13. CO_2 uptake (%) of different mixes

3.7 Cost analysis of biochar concrete

In the concrete mixes studied, the proportions of cement and biochar were systematically varied, revealing a significant impact on both the cost and environmental performance. **Table 7** shows the cost analysis of the control and biochar concrete with different percentages. As biochar was introduced into the mix at increasing levels (M5, M10, and M15), the overall cost of the concrete increased significantly compared with that of the control mix (M0), which contained no biochar. The cost of M0 is Rs. 4248.8 per cubic meter, whereas M5, M10, and M15 cost Rs. 4386.44, Rs. 4524.08, and Rs. 4661.72 per cubic meter, respectively. This cost escalation is driven by the high unit price of biochar (Rs. 15/kg) and its increasing inclusion in the mix, replacing a portion of the cement, which is less expensive (Rs. 7.6/kg). Additionally, the costs of fine and coarse aggregates remained constant across all mixes, highlighting the specific cost impact of biochar substitution. The unit cost of biochar depends on its supplier and quality. This will vary from place to place. In this study, the cost was higher because of the lack of standardization and cost efficiency in biochar production.

Table 7. Cost analysis of different concrete mixes

Material	Unit cost (Rs. /kg)	Cost (Rs. /m^3)			
		M0	M5	M10	M15
Cement	7.6	2827.2	2685.84	2544.48	2403.12
Biochar	15	-	279	558	837
Fine aggregate	0.55	407.55	407.55	407.55	407.55
Coarse aggregate	0.85	1014.05	1014.05	1014.05	1014.05
Total cost		4248.8	4386.44	4524.08	4661.72

Cement production represents a significant source of global carbon emissions, accounting for approximately 8% of worldwide CO_2 output. The integration of biochar into concrete offers a transformative pathway to offset these emissions through dual carbon sequestration mechanisms. Biochar sequesters carbon directly during pyrolysis by capturing atmospheric carbon and converting it into a stable form that persists for 100+ years. When incorporated into concrete at 5% replacement levels, biochar facilitates further sequestration through carbonation, wherein carbon dioxide reacts with the concrete matrix over time, creating additional carbon sinks. This dual mechanism of carbon capture enables biochar-concrete to transition from a high-carbon material to a carbon-negative solution, fundamentally reframing the role of construction materials in climate mitigation.

Despite the promising technical performance of 5% biochar in cement composites, its higher cost remains a significant barrier to commercial adoption. However, several complementary strategies can accelerate market penetration: (1) government subsidies for low-carbon construction materials and agricultural waste valorization; (2) green building certification credits (LEED, GRIHA) for using carbon-negative materials; (3) industrial scaling of biochar production to reduce costs through economies of scale; (4) development of standardized specifications for biochar in construction to build industry confidence; and (5) integration into national climate action plans as a recognized carbon sequestration technology. Future policy frameworks should explicitly include biochar-concrete as an eligible carbon-negative construction material to incentivize wider adoption. When contextualized within biochar's remarkable environmental advantages, multiple policy incentives and industrial strategies are emerging to offset this economic challenge.

Among the most powerful economic levers, carbon credit mechanisms represent one of the most viable revenue streams for closing the cost gap. Biochar is currently priced at \$100–\$250 per ton of CO_2 equivalent in voluntary carbon markets, substantially higher than conventional carbon credit prices due to its exceptional permanence (100+ years) and multiple co-benefits [46, 47]. These high-integrity carbon credits are particularly attractive to corporations pursuing net-zero commitments; for example, Microsoft purchased 60,000 tons of biochar carbon credits in Q2 2024 as part of its strategy to achieve carbon-negative status by 2030 [48]. Complementing market-based carbon revenues, direct policy support at the governmental level is actively subsidizing biochar deployment costs. The United States Department of Agriculture offers direct financial assistance through the Environmental Quality Incentives Program (EQIP), specifically through Conservation Practice Standard Code 336, which provides \$200 per acre incentive payments for biochar application, effectively subsidizing a portion of material costs[46, 49]. Similarly, the USDA Rural Development program offers grants up to 25% of project costs through the Rural Energy for America Program (REAP) and loan guarantees up to \$250 million through the Biorefinery and Renewable Chemical Manufacturing Assistance Program for biochar production facilities [50]. In the European Union, economic modeling indicates that higher carbon subsidies ranging from 183 to 812 EUR per ton of CO_2 equivalent would be required to make biochar economically viable at current production costs, underscoring the need for region-specific policy support explicitly tailored to construction applications [51].

Beyond policy interventions, industrial strategies focused on economies of scale and technological optimization are systematically reducing production costs. European biochar production is growing at 50% annually, and projections indicate unit costs will decline substantially with increased demand and automation [52]. At the industrial level, biochar integration into cement production as a partial clinker substitute and into steel manufacturing creates synergies that improve overall project economics while multiplying carbon sequestration benefits. Cost-benefit analyses demonstrate that effective CO_2 reduction costs for biochar integration range from \$100–\$200 per ton when combined with carbon credit revenue, compared to \$500–\$800 per ton for hydrogen-based decarbonization alternatives [53]. This cost advantage positions biochar as one of the most economically competitive pathways for hard-to-abate sectors. Further strengthening the economic case, circular economy strategies that valorize agricultural and forestry residues as biochar feedstocks provide additional economic leverage. By eliminating or substantially reducing feedstock costs, these approaches create additional revenue streams that can subsidize biochar production and offset application expenses while simultaneously supporting rural economies [54]. For construction applications, coupling residue-based feedstocks with local concrete markets can shorten supply chains, reduce transportation emissions, and strengthen the overall environmental performance profile while distributing economic benefits across agricultural and construction value chains.

The commercialization pathway is further supported by voluntary carbon market maturation, where high-integrity biochar projects now command premium prices as corporate buyers increasingly demand credible carbon removal certificates meeting Core Carbon Principles standards [55]. Public-private partnerships and industry roadmaps—such as those developed by the International Biochar Initiative's 2024–2030 Strategic Plan—are establishing pathways to mainstream biochar into construction codes, product standards, and procurement guidelines, thereby creating predictable demand that encourages private investment and accelerates cost reduction [56]. Ultimately, while the higher upfront cost of biochar-amended concrete currently presents an adoption barrier, the convergence of carbon credits, direct subsidies, technological improvements, circular economy benefits, and dual carbon sequestration mechanisms positions 5% biochar integration as an economically viable and environmentally transformative solution. As carbon pricing matures and policy support expands, biochar-concrete has the potential to fundamentally decarbonize the construction industry while generating measurable environmental and economic value, making the initial cost premium a strategic investment rather than a burden. Within the next 3–5 years, market dynamics, regulatory incentives, and demonstrated climate impact are expected to render biochar adoption not merely economically competitive, but economically compelling for sustainable construction practices globally.

4 Conclusions

The experimental investigation of activated bamboo biochar as a cement replacement in M20 concrete has yielded significant findings that advance understanding of biochar-enhanced cementitious materials while simultaneously addressing critical questions regarding optimal dosage and practical feasibility. The 5% biochar replacement emerges as the optimal dosage for this activated bamboo biochar system, representing a balance between mechanical performance, durability, environmental benefit, and structural integrity that is distinctly different from prior studies reporting 1–3% as optimal. This distinction reflects the unique combination of steam-activated biochar material properties, controlled concrete mix design, and the specific testing framework employed in this research.

The concrete mix design employed in this study maintains a constant water-to-binder (w/b) ratio of 0.50 across all mixes (M0, M5, M10, M15), isolating intrinsic physical mechanisms contributed by activated biochar while controlling for confounding variables. The experimental results decisively establish 5% as optimal: compressive strength at M5 showed 34.30 MPa at 120 days (1.84% improvement over control); split tensile strength at M5 showed 8.08% improvement (3.75 MPa versus 3.47 MPa); EDS revealed highest calcium and silicon content at M5, supporting C-S-H formation; Ultrasonic Pulse Velocity improved by 1.04% at M5 indicating enhanced homogeneity. Water penetration depth at M5 (4.2 mm) maintained acceptable durability, and carbon sequestration capacity at 5% reached 37.01%—a reasonable compromise between environmental benefit and structural performance.

Policy incentives including carbon credits (\$100–\$250 per ton CO_2 equivalent) and USDA EQIP subsidies (\$200 per acre) establish 5% as economically viable despite higher biochar expenses. The dual carbon sequestration mechanism—capturing atmospheric carbon during pyrolysis and facilitating further CO_2 uptake through concrete carbonation—enables 5% biochar-concrete to transition from high-carbon to carbon-negative material.

Future research should prioritize: (i) Comprehensive Life Cycle Cost Analysis (LCCA) accounting for biochar production emissions, transportation, and long-term durability benefits to establish true economic viability; (ii) Pozzolanic activity characterization through strength activity index (SAI) and chemical analysis (XRF, XRD) to quantitatively validate cement hydration mechanisms; (iii) Comparative benchmarking against established SCMs (fly ash, slag, silica fume) under identical testing conditions to clarify competitive advantages; (iv) Extended durability testing beyond 120 days monitoring carbonation, chloride penetration, and freeze-thaw resistance; (v) Industrial-scale assessment examining production optimization, feedstock supply chain, and standardization requirements; and (vi) Field-scale pilot projects with in-situ monitoring and real-world cost tracking to validate findings and facilitate regulatory acceptance. These coordinated efforts would bridge laboratory validation to market implementation, enabling widespread adoption of biochar concrete in sustainable construction.

Acknowledgement

The authors would like to express their sincere gratitude to the Rajarambapu Institute of Technology, Islampur, India, for providing seed funding, which made this research possible. The authors also acknowledge the support of the Civil Engineering Department for access to laboratory facilities and technical assistance during the experimental work. Special thanks are extended to the faculty mentors and staff members who contributed their insights and encouragement throughout the project.

Funding Statement

This research was supported by the Rajarambapu Institute of Technology, Islampur, India, through a seed funding scheme.

CRediT authorship contribution statement

Afan Tamboli: Conceptualization, Methodology, Experimental Investigation, Visualization, Data Analysis, Writing-Original Draft. **Sourabh Patil:** Literature Review, Laboratory Work, Experimental Investigation. **Mayur Maske:** Supervision, Methodology Guidance, Writing – Review & Editing. **Savita Patil:** Project Administration, Validation, Funding Acquisition. **Sabir Sayyed:** Technical Guidance, Writing – Review & Editing.

Conflicts of Interest

The authors declare that they have no conflicts of interest to report regarding the present study.

Data Availability Statement

Some or all data, models, or codes that support the findings of this study are available from the corresponding author upon reasonable request.

References

[1] Khaiyum MZ, Kabir G, Sarker S. Evaluation of carbon emission factors in the cement industry: an emerging economy context. Sustainability 2023; 15(21): 15407. https://doi.org/10.3390/su152115407.

[2] Sousa V, Real S, Bogas JA, Meireles I. Industrial production of recycled cement: energy consumption and carbon dioxide emission estimation. Environmental Science and Pollution Research 2022; 30(4): 8778–8789. https://doi.org/10.1007/s11356-022-20887-7.

[3] Da Silva Rego JH, Visedo G, Mora P, Zaragoza A, Sanjuán MÁ. Carbon dioxide uptake by Brazilian cement-based materials. Applied Sciences 2023; 13(18): 10386. https://doi.org/10.3390/app131810386.

[4] Gao X, Zhang Y, Qi X, Liao C. A scenario simulation of material substitution in the cement industry under the carbon neutral strategy: a case study of Guangdong. Sustainability 2023; 15(7): 5736. https://doi.org/10.3390/su15075736.

[5] Zhou C, Luo X, Liu W, Xuan D, Miao Y, Zhang Y. Accounting CO2 emissions of the cement industry: based on an electricity-carbon coupling analysis. Energies 2023; 16(11): 4453. https://doi.org/10.3390/en16114453

[6] Abiodun YO, Ochulor EF, Gbenebor OP, Obasa DV, Olanrewaju OA, Adeosun SO. Cutting cement industry CO2 emissions through metakaolin use in construction. Atmosphere 2022; 13(9): 1494. https://doi.org/10.3390/atmos13091494.

[7] Cheng D, Reiner DM, Yang F, Cui C, Meng J, Shan Y, Liu Y, Tao S, Guan D. Projecting future carbon emissions from cement production in developing countries. Nature Communications 2023; 14(1). https://doi.org/10.1038/s41467-023-43660-x.

[8] Poudyal L, Adhikari K. Environmental sustainability in cement industry: an integrated approach for green and economical cement production. Resources, Environment and Sustainability 2021; 4: 100024. https://doi.org/10.1016/j.resenv.2021.100024.

[9] Ramos R, Peixoto AF, Fernandes DM, Matos R, Abdelkader-Fernández VK. Metal-supported biochar catalysts for sustainable biorefinery, electrocatalysis, and energy storage applications: a review. Catalysts 2022; 12(2): 207. https://doi.org/10.3390/catal12020207.

[10] Hussain R, Ravi K, Garg A. Soil-biochar-plant interaction: differences from the perspective of engineered and agricultural soils. Bulletin of Engineering Geology and the Environment 2020; 79(9): 4461–4481. https://doi.org/10.1007/s10064-020-01846-3.

[11] Torabian S, Lu Y, Qin R, Wang G, Noulas C. Biochar: an organic amendment to crops and an environmental solution. AIMS Agriculture and Food 2021; 6(1): 401–415. https://doi.org/10.3934/agrfood.2021024.

[12] Ling Y, Wu X, Zou Z, Tan K. Effect of biochar dosage and fineness on the mechanical properties and durability of concrete. Materials 2023; 16(7): 2809. https://doi.org/10.3390/ma16072809.

[13] Aman AMN, Chen WH, Selvarajoo A, Lau TL. Biochar as a cement replacement to enhance concrete composite properties: a review. Energies 2022; 15(20): 7662. https://doi.org/10.3390/en15207662.

[14] Yosri AM, Zaid O, Hamad M. Valorization of engineered biochar to develop ultra-high-performance fiber-reinforced concrete with low carbon emission. Journal of Sustainable Cement-Based Materials 2024; 13(6): 865–887. https://doi.org/10.1080/21650373.2024.2333270.

[15] Liu W, Li K, Xu S. Utilizing bamboo biochar in cement mortar as a bio-modifier to improve the compressive strength and crack-resistance fracture ability. Construction and Building Materials 2022; 327: 126917. https: //doi.org/10.1016/j.conbuildmat.2022.126917.

[16] Khan K, Zubair M, Amin MN, Aziz MA. Biochar produced from Saudi agriculture waste as a cement additive for improved mechanical and durability properties-SWOT analysis and techno-economic assessment. Materials 2022; 15(15): 5345. https://doi.org/10.3390/ma15155345.

[17] Beskopylny AN, Stel'Makh SA, Meskhi B, Mailyan LR, Smolyanichenko AS, Beskopylny N, Shcherban' EM. High-performance concrete nanomodified with recycled rice straw biochar. Applied Sciences 2022; 12(11): 5480. https://doi.org/10.3390/app12115480.

[18] Turovaara M. The effect of high-ratio biochar replacement in concrete on performance properties: experimental study of biochar addition to concrete mixture. DIVA 2022.

[19] Patel R, Stobbs J, Acharya B. Study of biochar in cementitious materials for developing green concrete composites. Scientific Reports 2025; 15(1): 22192. https://doi.org/10.1038/s41598-025-07210-3.

[20] Gupta S, Kua HW, Pang SD. Biochar-mortar composite: manufacturing, evaluation of physical properties and economic viability. Construction and Building Materials 2018; 167: 874–889. https://doi.org/10.1016/j.conbuildmat.2018.02.104.

[21] Sacdalan JLD, Bartolo CAD, Bautista CAD, Cruz GG, Muñoz JC. Bamboo-derived biochar as partial cement replacement in concrete for carbon dioxide capturing and sequestration. Chemical Engineering Transactions 2023; 106: 409–414.

[22] Sirico A, Bernardi P, Sciancalepore C, Vecchi F, Malcevschi A, Belletti B, Milanese D. Biochar from wood waste as additive for structural concrete. Construction and Building Materials 2021; 303: 124500. https://doi.org/10.1016/j.conbuildmat.2021.124500.

[23] Barbhuiya S, Das BB, Kanavaris F. Biochar-concrete: a comprehensive review of properties, production and sustainability. Case Studies in Construction Materials 2024; 20: e02859. https://doi.org/10.1016/j.cscm.2024.e02859.

[24] Wu F, Zhang Q, Dong S, Cai Y, Yang S, Xu F, Luo P, Jiang J. Biochar modification enhances mechanical and durability properties of cement-based materials. Scientific Reports 2025; 15(1): 22174. https://doi.org/10.1038/s41598-025-06968-w.

[25] Gunasekaran PK, Chin SC. Performance of bamboo biochar as partial cement replacement in mortar. Materials Today Proceedings 2023; 109: 53–61. https://doi.org/10.1016/j.matpr.2023.06.322.

[26] Bureau of Indian Standards. IS 10262: Concrete mix proportioning—Guidelines. 2nd rev. New Delhi: BIS 2019.

[27] Bureau of Indian Standards. IS 4031:1988 - Methods of physical tests for hydraulic cement. New Delhi: BIS 1988.

[28] Bureau of Indian Standards. IS 2185 (Part 1):2005 - Concrete masonry units: Specification. New Delhi: BIS 2005.

[29] Bureau of Indian Standards. IS 1199:1959 - Methods of sampling and analysis of concrete. New Delhi: BIS 1959.

[30] Bureau of Indian Standards. IS 516:1959 - Method of tests for strength of concrete. New Delhi: BIS; 1959.

[31] Bureau of Indian Standards. IS 5816:1999 - Splitting tensile strength of concrete: method of test. New Delhi: BIS 1999.

[32] Kumbhar SS, Patil SN, Maske MM, Sayyed SS. Performance analysis of self-compacting fiber reinforced concrete with e-waste fibers at various elevated temperatures. Multiscale and Multidisciplinary Modeling Experiments and Design 2024. https://doi.org/10.1007/s41939-024-00579-0.

[33] Bureau of Indian Standards. IS 13311 (Part 1):1992 - Methods of non-destructive testing of concrete. New Delhi: BIS 1992.

[34] Bureau of Indian Standards. IS 516 (Part 5/Section 3): Hardened concrete—Methods of test—Part 5: Non-destructive testing—Section 3: Carbonation depth test. New Delhi: BIS.

[35] Nair JJ, Shika S, Sreedharan V. Biochar amended concrete for carbon sequestration. IOP Conference Series: Materials Science and Engineering 2020; 936(1): 012007. https://doi.org/10.1088/1757-899x/936/1/012007.

[36] Neve S, Sarkar D, Meng W, Bao Y, Barhemat R, Du J. Valorization of Vetiver root biochar in eco-friendly reinforced concrete: mechanical, economic, and environmental performance. Materials 2023; 16(6): 2522. https://doi.org/10.3390/ma16062522

[37] Sinha S, Pandey A, B SN, Prasad B. Prelim.inary study of agricultural waste as biochar incorporated into cementitious materials. Journal of Architectural Environment & Structural Engineering Research 2023; 6(2): 59–79. https://doi.org/10.30564/jaeser.v6i2.5695.

[38] Gupta S, Kua HW, Pang SD. Effect of biochar on mechanical and permeability properties of concrete exposed to elevated temperature. Construction and Building Materials 2019; 234: 117338. https://doi.org/10.1016/j.conbuildmat.2019.117338.

[39] Akhtar A, Sarmah AK. Novel biochar-concrete composites: manufacturing, characterization and evaluation of the mechanical properties. Science of The Total Environment 2017; 616-617: 408–416. https://doi.org/10.1016/j.scitotenv.2017.10.319.

[40] Cuthbertson D, Berardi U, Briens C, Berruti F. Biochar from residual biomass as a concrete filler for improved thermal and acoustic properties. Biomass and Bioenergy 2018; 120: 77–83. https://doi.org/10.1016/j.biombioe.2018.11.007.

[41] Li Z, Xue W, Zhou W. Mechanical properties of concrete with different Carya cathayensis peel biochar additions. Sustainability 2023; 15(6): 4874. https://doi.org/10.3390/su15064874.

[42] Zeidabadi ZA, Bakhtiari S, Abbaslou H, Ghanizadeh AR. Synthesis, characterization and evaluation of biochar from agricultural waste biomass for use in building materials. Construction and Building Materials 2018; 181: 301–308. https://doi.org/10.1016/j.conbuildmat.2018.05.271.

[43] Gupta S, Kua HW. Application of rice husk biochar as filler in cenosphere modified mortar: preparation, characterization and performance under elevated temperature. Construction and Building Materials 2020; 253: 119083. https://doi.org/10.1016/j.conbuildmat.2020.119083.

[44] Gupta S, Kua HW. Effect of water entrainment by pre-soaked biochar particles on strength and permeability of cement mortar. Construction and Building Materials 2017; 159: 107–125. https://doi.org/10.1016/j.conbuildmat.2017.10.095.

[45] Yang X, Wang X. Hydration-strength-durability-workability of biochar-cement binary blends. Journal of Building Engineering 2021; 42: 103064. https://doi.org/10.1016/j.jobe.2021.103064.

[46] Anaxee. How biochar carbon credits work: from production to climate impact 2025; 22(25). https://anaxee.com/biochar-carbon-credits/.

[47] Sustainability Directory. Policy frameworks for biochar in agriculture and carbon sequestration 2025; 04 (25)https://prism.sustainability-directory.com/scenario/policy-frameworks-for-biochar-in-agriculture-and-carbon-sequestration/.

[48] BX Tech. Biochar carbon credits: how farmers can turn waste into wealth 2024; 15 (25). https://bx.tech/insights/biochar-carbon-credits-how-farmers-can-turn-waste-into-wealth/.

[49] Advanced Agrilytics. New EQIP practice offers incentive payments for biochar applications 2025; 30 (25). https://advancedagrilytics.com/new-eqip-practice-offers-incentive-payments-for-biochar-applications/.

[50] Jozana Grants. Biochar grants 2025; 27 (25). https://jozanagrants.com/biochar-grants/.

[51] Jokubė M, et al. Economic feasibility of biochar for carbon stock increase in Finnish mineral agricultural soil. Taylor & Francis Online 2025; 14(6). https://www.tandfonline.com/doi/full/10.1080/17583004.2025.24653251.

[52] Deng X, et al. Exploring negative emission potential of biochar to achieve climate targets. Nature Communications 2024; 15: 1234. https://www.nature.com/articles/s41467-024-45314-y.

[53] Environmental Science & Technology. Breaking the carbon barrier: engineered biochar as industrial decarbonisation solution. IJMER 2023; 14(6): 67–99. http://mail.ijmer.com/papers/Vol14_issue6/14067299.pdf.

[54] Lehmann J, et al. Biochar in the circular bionutrient economy. Proceedings of the National Academy of Sciences 2025; 122(33): e2503668122. https://www.pnas.org/doi/10.1073/pnas.2503668122.

[55] ReGreener Earth. Voluntary carbon market: latest prices and developments 2025; 2 (30). https://www.regreener.earth/blog/voluntary-carbon-market-update, Oct.

[56] International Biochar Initiative. Strategic plan 2024-2030 2024; 26 (25). https://biochar-international.org/strategic-plan-2024-2030/.